Arch. Metall. Mater. **68** (2023), 2, 563-569

DOI: https://doi.org/10.24425/amm.2023.142435

A. VAŠKO[1*], M. UHRÍČIK[1], V. KAŇA[2]

FATIGUE RESISTANCE AND OTHER UTILITY PROPERTIES OF NiMn-TYPE OF AUSTENITIC NODULAR CAST IRON

The aim of this paper is to evaluate the fatigue resistance of austenitic nodular cast iron and to compare it with other types of nodular cast irons. The austenitic nodular cast iron, used for the experiments, was alloyed by 13% nickel and 7% manganese (EN-GJSA-XNiMn13-7) to obtain an austenitic matrix. The microstructure was studied using light metallographic microscopy. Mechanical properties were investigated by tensile test, impact bending test and Brinell hardness test. Fatigue tests were carried out at sinusoidal cyclic push-pull loading at ambient temperature. The results of fatigue tests were compared with the fatigue properties of ferrite-pearlitic nodular cast iron and pearlite-ferritic nodular cast iron. Experimental results show that NiMn-type of austenitic nodular cast iron has lower tensile strength and hardness, but higher elongation and absorbed energy than the compared types of nodular cast iron. However, austenitic nodular cast iron has lower fatigue limit.

Keywords: Ni-Resist; austenitic nodular cast iron; EN-GJSA-XNiMn13-7; fatigue; push-pull loading

1. Introduction

Nodular cast iron is characterized by high strength, elongation, fatigue resistance, resistance to shock, wear and corrosion. Other advantages, such as the ability to produce products of various sizes with complex geometries, as well as good castability and machinability and a high rate of recycling, make nodular cast iron an economical material in many applications [1,2].

Austenitic nodular cast iron is defined as a range of high-alloyed cast material with an austenitic matrix, containing nickel, manganese and sometimes also copper or chromium for stabilization of the austenitic matrix at room temperature. Carbon is contained in the material in the form of graphite nodules. Formation of austenite takes place under the influence of specific alloying elements, predominantly nickel, which decrease the eutectoid decomposition temperature of austenite to below room temperature. Materials with nickel contents of 15 to 36% are also grouped by the designation Ni-Resist [3,4].

Austenitic nodular cast irons are standardized according to STN EN 13835. This European standard specifies 10 grades of nodular cast iron and their chemical composition, required structure, mechanical properties (yield strength, tensile strength, elongation, impact energy and Brinell hardness) and physical properties. However, the standard does not prescribe the fatigue properties of these nodular cast irons.

For the experiments, austenitic nodular cast iron alloyed by nickel and manganese, designated EN-GJSA-XNiMn13-7, was chosen.

Nickel is the main alloying element in austenitic nodular cast irons. A nickel content of about 20% is required to maintain the stability of austenite at low temperatures. This content is higher than that of conventional stainless steels. This is necessary because the support effect of high chromium content is lacking. Chromium can only be used in limited quantities in graphitic cast iron, otherwise excessive carbide formation would cause increased hardness and thus difficulties in machining, embrittlement and deterioration of foundry properties. In certain circumstances (mainly for economic reasons) part of the nickel may be replaced by other elements stabilizing austenite, e.g. manganese or copper [5]. The price of manganese is significantly lower than the price of nickel, so replacing part of the nickel with manganese has a significant economic benefit for some grades of austenitic cast irons [6]. However, manganese does not contribute to corrosion or heat resistance, it is only used in higher concentrations in non-magnetizable or cold-resistant types. Copper can be used as a substitute for nickel only in lamellar cast

[1] UNIVERSITY OF ŽILINA, FACULTY OF MECHANICAL ENGINEERING, DEPARTMENT OF MATERIALS ENGINEERING, ŽILINA, SLOVAKIA
[2] BRNO UNIVERSITY OF TECHNOLOGY, FACULTY OF MECHANICAL ENGINEERING, DEPARTMENT OF FOUNDRY ENGINEERING, BRNO, CZECH REPUBLIC
* Corresponding author: alan.vasko@fstroj.uniza.sk

iron, but not in nodular cast iron, because it prevents the formation of nodular graphite. The content of nickel, chromium and manganese can be summarized in nickel equivalent according to the Eq. (1) [5].

$$\text{nickel equivalent} = \%Ni + 2 \cdot \%Mn + \%Cr > 23.5\% \quad (1)$$

In cases where a stable austenitic structure below room temperature is required, a nickel equivalent of at least 23.5% is necessary. However, instability is usually not a problem, so the nickel content is at the lower end of the normal range for cost reasons. Due to the possible loss of nickel in the segregation zones, a slightly higher nickel content should be set for larger wall thicknesses.

Manganese is an effective stabilizer of austenite, but does not contribute to corrosion or heat resistance, so it is used as a substitute for nickel only in non-magnetizable grade GJSA-XNiMn13-7. If corrosion resistance is also important, grades with low manganese and chromium content must be chosen [5]. The addition of 4% Mn increases the austenite stability so that applications at sub-zero temperatures are possible. The partial replacement of nickel by 7% Mn produces a cost-effective non-magnetizable nodular cast iron and avoids the ferromagnetic austenite field at high nickel contents [7].

Austenitic nodular cast iron is generally characterized by high resistance to elevated temperature, as well as low temperature, good corrosion resistance with exposure to sea water and alkaline media, erosion resistance, high elongation and it is not magnetizable. NiMn-type of nodular cast iron is used for non-magnetizable castings, e.g. pressure covers for turbochargers, housings for switching systems, insulating flanges, clamps, feedthroughs [8-10]. Some of these components are exposed to fatigue stress, so it is necessary to know their fatigue resistance, or look for ways to increase the fatigue characteristics of these parts.

Several articles, e.g. [11-19] deal with the relationship between chemical composition, structure, mechanical properties, heat or corrosion resistance of austenitic nodular cast irons, but just a few of them deal with the fatigue properties. For this reason, the paper deals with the fatigue resistance of austenitic nodular cast iron.

2. Experimental material and methods

Austenitic nodular cast iron alloyed by 13% nickel and 7% manganese was used for the experiments. According to the STN EN 13835, designation of this grade of nodular cast iron is EN-GJSA-XNiMn13-7 by symbol and 5.3506 by number. Casting process was realised in the foundry at the Department of Foundry Engineering at Brno University of Technology. Melting was carried out in an electric induction furnace. Modification and inoculation took place in a casting ladle by the sandwich method. Then, the melt was cast in the form of Y-shaped blocks into sand moulds (Fig. 1).

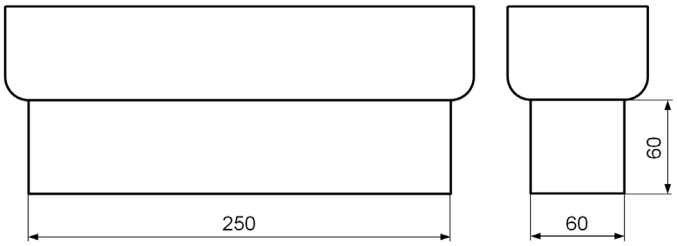

Fig. 1. Shape and dimensions of the cast Y blocks

The charge composition of the melt is given in TABLE 1. The basic charge consisted of steel, pig iron and additives for adjustment of chemical composition (content of carbon, silicon, nickel and manganese), i.e. carburizer, ferrosilicon FeSi75, nickel and ferromanganese FeMn80. Modification and inoculation were performed using FeSiMg7 modifier and FeSi75 inoculant. Content of the charge materials was chosen to achieve required chemical composition and austenitic matrix. The resulting chemical composition of the melt is given in TABLE 2.

Specimens for metallographic analysis, mechanical tests (tensile test, impact bending test, hardness test) and fatigue tests were made by machining from Y-blocks. Three cylindrical test specimens with a diameter d_0 = 10 mm and gauge length l_0 = 50 mm were used for tensile test. Three test specimens of square cross-section with a width a_0 = 10 mm and length l_0 = 55 mm without notch were used for impact bending test. These specimens were also used for hardness test, which was carried out

TABLE 1

Charge composition of the melt

Charging raw materials (kg)						Modifier & inoculant (kg)		
steel	pig iron	carburizer	FeSi75	Ni	FeMn80	modifier FeSiMg7	inoculant FeSi75	cover plates
23.5	17.5	0.7	1.7	7.8	5.5	0.7	0.4	3.0

TABLE 2

Chemical composition of EN-GJSA-XNiMn13-7 (5.3506)

	Content of chemical elements (weight %)											C_E
	C	Si	Mn	P	S	Cr	Ni	Cu	Mo	Al	Mg	
required	max 3.00	2.00-3.00	6.00-7.00	max 0.08	—	max 0.20	12.0-14.0	max 0.50	—	—	—	—
real	2.634	2.177	6.365	0.035	< 0.015	0.061	13.45	0.038	0.024	0.026	0.094	3.82

* Carbon equivalent C_E = %C + 0.33 %Si + 0.047 %Ni – (0.0055 %Ni × %Si)

at 5 different locations. 15 test specimens of circular cross-section with a diameter d_0 = 8 mm were used for fatigue tests (Fig. 2a).

Metallographic analysis, mechanical and fatigue tests and microfractographic analysis were realised in laboratories at the Department of Materials Engineering at the University of Žilina.

Metallographic analysis was carried out on the light metallographic microscope Neophot 32; microstructure of the specimens was evaluated according to STN EN ISO 945 (STN 42 0461) and by automatical image analysis using software NIS Elements AR 5.20 [20].

Tensile test was performed using the testing machine Zwick Roell Z250 according to STN EN ISO 6892-1; yield strength $R_{p0,2}$, tensile strength R_m and elongation A were evaluated. Impact bending test was performed using the Charpy hammer PSW 300 according to STN EN ISO 148-1; absorbed energy K was evaluated. Brinell hardness test was performed using the hardness tester CV-3000LDB according to STN EN ISO 6506-1; hardness HBW 10/3000/10 was evaluated.

Fatigue tests were performed at low frequency sinusoidal cyclic push-pull loading (stress ratio R = –1) at frequency $f \approx 75$ Hz at ambient temperature ($T = 23 \pm 5$°C) using the fatigue testing machine Zwick/Roell Amsler 150HFP 5100 (Fig. 2b, 2c) according to STN 42 0362; the Wöhler curve (relationship between stress amplitude σ_a and number of cycles to failure N_f) and fatigue limit σ_c for $N = 10^7$ cycles were determined [21,22].

Microfractographic analysis was carried out on fracture surfaces of the specimens fractured by fatigue tests using the scanning electron microscope VEGA II LMU.

3. Experimental results and discussion

Metallographic analysis revealed that the microstructure of the specimen EN-GJSA-XNiMn13-7 (5.3506) consists of austenite and nodular graphite (Fig. 3). The austenitic matrix was achieved by addition of nickel and manganese. Graphite is

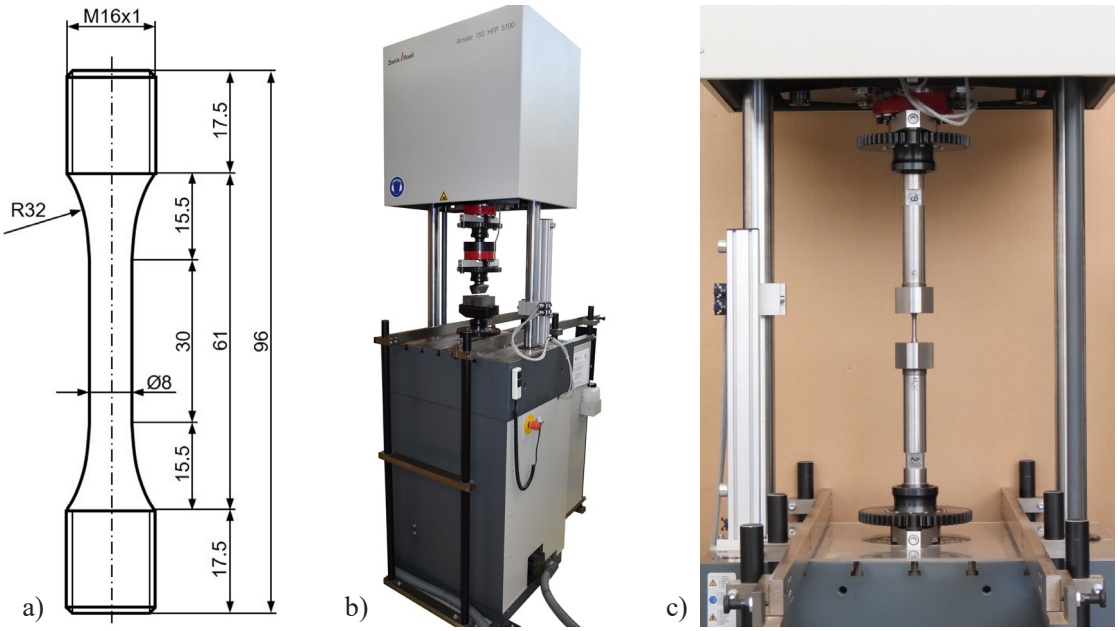

Fig. 2. Test specimen and experimental machine used for fatigue tests; a) shape and dimensions of the test specimen; b) fatigue testing machine Zwick/Roell Amsler 150HFP 5100; c) detail of fatigue testing

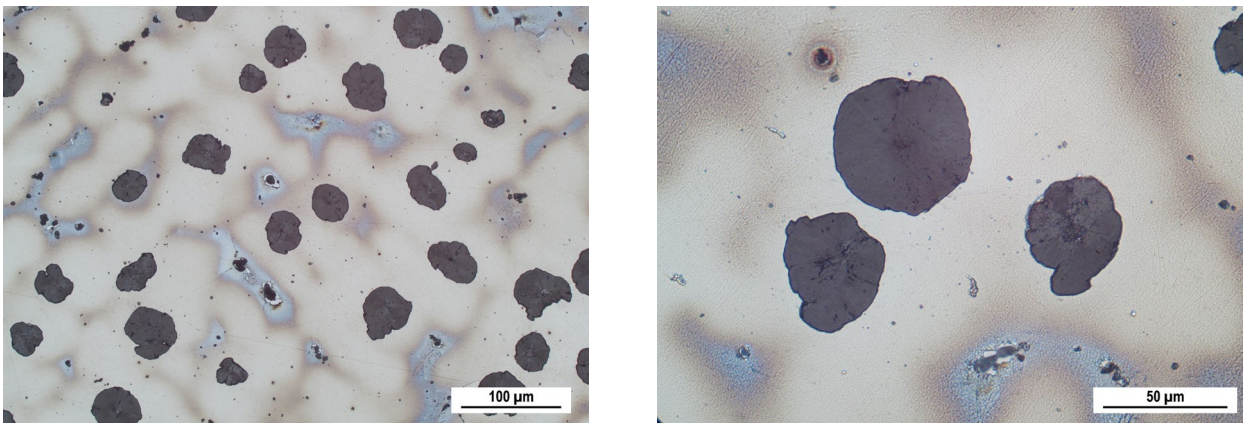

Fig. 3. Microstructure of austenitic nodular cast iron EN-GJSA-XNiMn13-7, etched by Kallins 2

present preferably in a perfectly spheroidal shape, only rarely occurs in an imperfectly spheroidal shape. The light blue areas in the matrix show the segregation of main elements (e.g. silicon, manganese, nickel) dissolved in the solid solution. Inclusions and impurities are also excluded in this area.

Results of quantitative evaluation of the microstructure according to a standard and by means of automatical image analysis are given in TABLE 3. Shape of graphite (designated by Roman numbers I to VI) and size of graphite (designated by numbers 1 to 8) were evaluated according to STN EN ISO 945, and shape factor, equivalent diameter of graphite, count of graphitic nodules per unit area and content of graphite were evaluated by image analysis.

According to STN EN ISO 945, graphite occurs in a perfectly spheroidal shape (80%) with a size of 30 to 60 μm and in an imperfectly spheroidal shape (20%) with the same size. According to image analysis, shape factor of graphite is 0.72, equivalent diameter of graphite is 36.3 μm, count of graphitic nodules is 78.1 mm^{-2} and content of graphite is 9.4%.

Microstructure has a direct effect on the mechanical properties, which were determined by tensile test, impact bending test and Brinell hardness test. Mechanical properties required by a standard and the measured mechanical properties are given in TABLE 4. Tensile curves obtained by tensile test, performed on three test specimens, are shown in Fig. 4. Yield strength $R_{p0,2}$ is 237.7 MPa, tensile strength R_m is 475.3 MPa, elongation A is 29.0%, reduction of area Z is 21.5%, absorbed energy K is 197.3 J (test specimens without notch) and Brinell hardness is 138.7 HBW10/3000/10. Measured mechanical properties correspond to those required by the standard.

Fatigue tests were performed at low frequency cyclic push-pull loading ($f \approx 75$ Hz) on 15 specimens. For all selected levels of stress amplitude, 2 or 3 specimens were used for higher accuracy of results. Wöhler fatigue curve was constructed from the measured values of stress amplitude σ_a and number of cycles to failure N_f (Fig. 5). Obtained data were approximated by the power function using the least square method [23]. From the fatigue curve, fatigue limit σ_c for $N = 10^7$ cycles and ratio of fatigue limit and tensile strength σ_c/R_m were determined. Fatigue limit is defined as the highest stress that the material can theoretically withstand an infinite number of cycles.

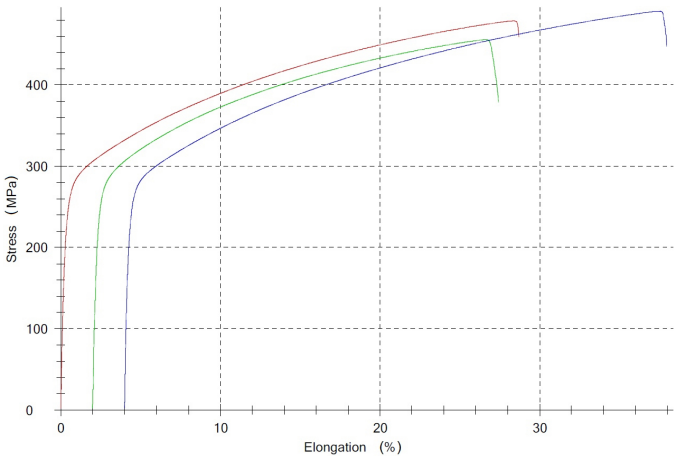

Fig. 4. Tensile curves of austenitic nodular cast iron EN-GJSA-XNiMn13-7

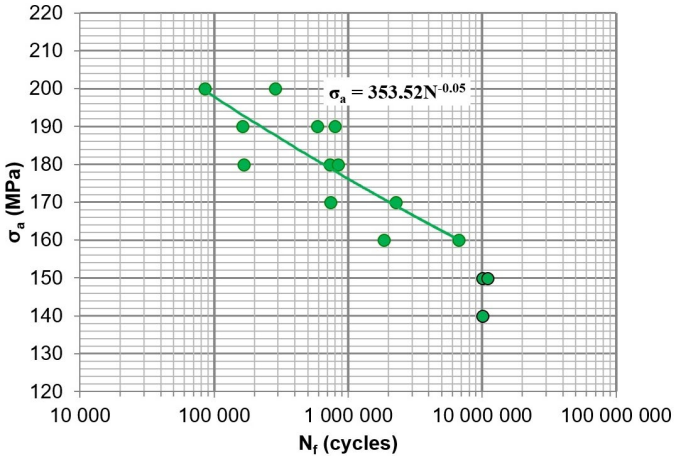

Fig. 5. Wöhler fatigue curve $\sigma_a = f(N)$ of austenitic nodular cast iron EN-GJSA-XNiMn13-7, σ_c = 150 MPa, σ_c/R_m = 0.32

The number of cycles to failure N_f increases with a decreasing stress amplitude σ_a. Fatigue tests show that the fatigue limit σ_c is 150 MPa and ratio of fatigue limit and tensile strength σ_c/R_m is 0.32.

The fatigue properties of austenitic nodular cast iron were compared with another two nodular cast irons with ferrite-

TABLE 3

Quantitative evaluation of the microstructure of austenitic nodular cast iron EN-GJSA-XNiMn13-7

Microstructure (according to STN EN ISO 945)	Shape factor of graphite *	Equivalent diameter of graphite (μm)	Count of graphitic nodules (mm^{-2})	Content of graphite (%)
80%VI6 + 20%V6	0.72	36.3	78.1	9.4

* Shape factor $S = \frac{4\pi A}{P^2}$, where A is an area and P is a perimeter of graphitic particles

TABLE 4

Mechanical properties of austenitic nodular cast iron EN-GJSA-XNiMn13-7

Property	$R_{p0.2}$ (MPa)	R_m (MPa)	A (%)	Z (%)	K0 (J)	HBW 10/3000/10
required	210-260	390-470	15-18	—	—	120-150
real	237.7	475.3	29.0	21.5	197.3	138.7

pearlitic and pearlite-ferritic matrix (Fig. 6). The first of them was alloyed by silicon and molybdenum (EN-GJS-X300SiMo4-1) and it is a ferrite-pearlitic nodular cast iron. The second one was alloyed by silicon and copper (EN-GJS-X300SiCu4-1.5) and it is a pearlite-ferritic nodular cast iron. The fatigue properties of both nodular cast irons were evaluated in the same way and under the same conditions than in the case of the austenitic nodular cast iron [24].

Comparison of fatigue properties shows that SiMo-grade and SiCu-grade of nodular cast irons have a higher fatigue limit σ_c than austenitic nodular cast iron, while SiCu-grade (σ_c = 270 MPa, σ_c/R_m = 0.41) has a higher fatigue limit and higher ratio of fatigue limit and tensile strength than SiMo-grade (σ_c = 210 MPa, σ_c/R_m = 0.37). Wöhler fatigue curves of these nodular cast irons are given in Fig. 6. The results of the fatigue tests indicate that the fatigue limit σ_c is related to the tensile strength R_m, i.e. the fatigue limit increases with increasing tensile strength.

Fatigue tests of all three types of nodular cast irons were carried out only at alternating symmetrical cyclic push-pull loading (medium stress of cycle σ_m = 0). However, this simple loading occurs relatively little in practice. Particular machine components are usually subjected to cyclic loading with a certain medium stress of cycle σ_m. In order to obtain a complete picture of the fatigue resistance, it would be necessary to perform fatigue tests at different values of medium stress σ_m and construct a diagram of the limit cycles. An alternative is to construct a Smith fatigue diagram which expresses the values of fatigue limit for individual types of cyclic loading (symmetrical, asymmetrical, disappearing, pulsating). The area of the diagram represents the field of safe loading of the component at different types of cyclic loading. If the applied load does not exceed this area, fatigue fracture will not occur under loading.

Simplified Smith fatigue diagrams for all three types of nodular cast iron are shown in Fig. 7. It is clear from the diagrams that the value of fatigue limit depends on the type of cyclic load-

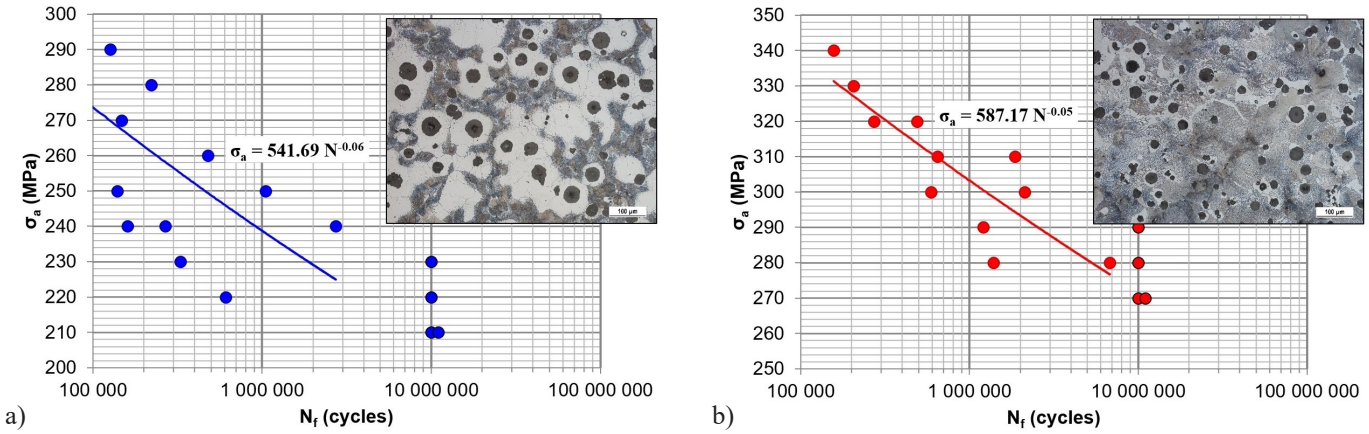

Fig. 6. Wöhler fatigue curves and microstructure of ferrite-pearlitic and pearlite-ferritic nodular cast irons; a) EN-GJS-X300SiMo4-1, R_m = 573.9 MPa, σ_c = 210 MPa, σ_c/R_m = 0.37; b) EN-GJS-X300SiCu4-1.5, R_m = 652.7 MPa, σ_c = 270 MPa, σ_c/R_m = 0.41

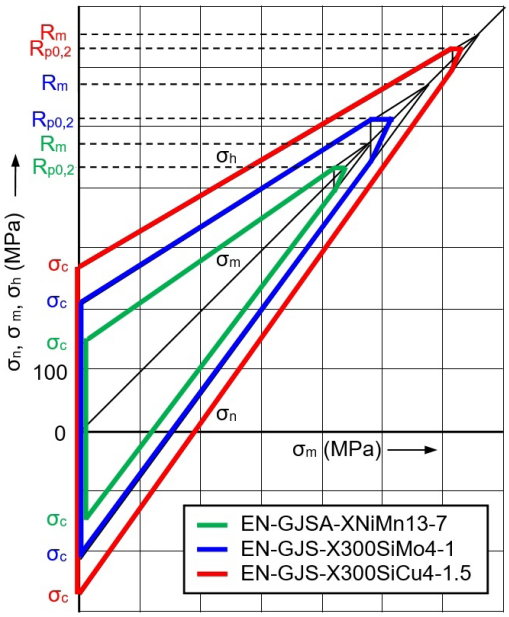

Fig. 7. Smith fatigue diagrams of austenitic (NiMn-grade), ferrite-pearlitic (SiMo-grade) and pearlite-ferritic (SiCu-grade) nodular cast irons

ing (symmetrical, asymmetrical, disappearing, pulsating). The alternating symmetrical cycle has the smallest absolute value of fatigue limit σ_c. With increasing medium stress σ_m, the absolute value of fatigue limit $\sigma_c = \sigma_m + \sigma_a$ increases, but at the same time its largest stress amplitude σ_a decreases.

Comparison of all three diagrams (Fig. 7) shows that SiMo-grade and SiCu-grade of nodular cast irons have a significantly larger area of the Smith fatigue diagram than austenitic nodular cast iron, therefore they also have a higher fatigue resistance at different types of cyclic loading. SiCu-grade has a larger area of the Smith fatigue diagram than SiMo-grade.

After fatigue tests, microfractographic analysis of selected specimens of austenitic nodular cast iron was performed. Micromechanisms of failure of the specimens broken under fatigue stress are shown in Fig. 8. A general view of the fracture surface after fatigue failure is captured in Fig. 8a, where it is possible to distinguish the area of propagation of the fatigue crack from the more fragmented area of final rupture. The fatigue fractures were initiated by a cavity (casting defect) which acted as a primary notch (Fig. 8b) or by a crack under the surface (Fig. 8c).

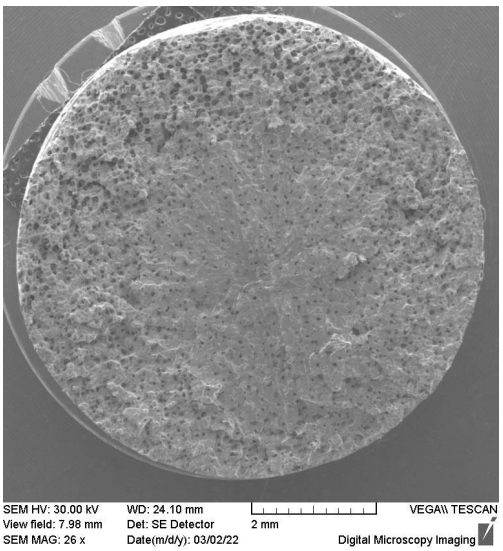

a)

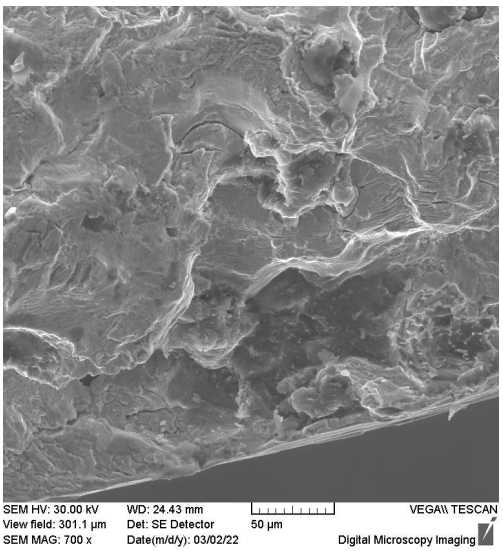

b)

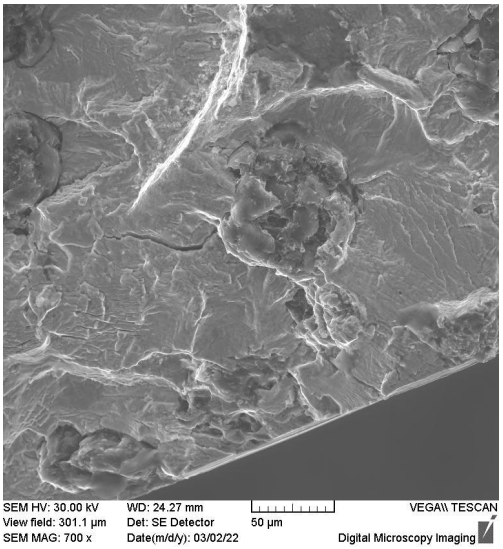

c)

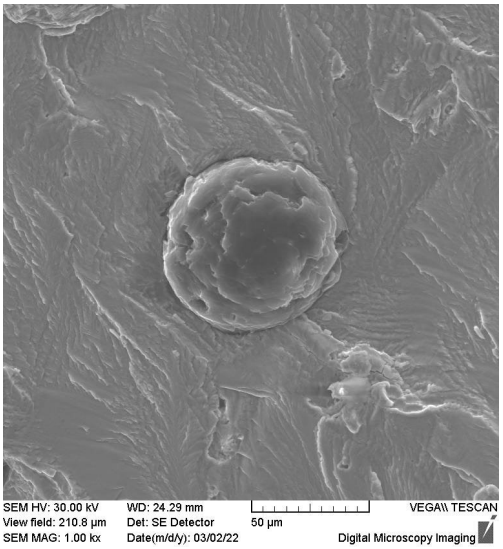

d)

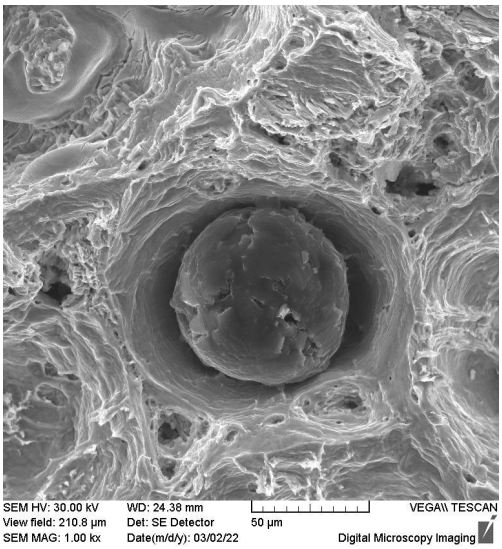

e)

Fig. 8. Fracture surfaces of analysed specimens; a) general view of fracture surface after fatigue failure; b) initiation of fatigue failure by a casting defect; c) initiation of fatigue failure by a crack under the surface; d) transcrystalline fatigue failure; e) transcrystalline ductile failure in the area of final rupture

The fatigue fracture is characteristic of transcrystalline fatigue failure of austenite (Fig. 8d); intercrystalline fatigue failure was not observed. The area of final rupture is characteristic of transcrystalline ductile failure with dimple morphology (Fig. 8e); transcrystalline cleavage of matrix occures only rarely.

Micromechanisms of fatigue failure of austenitic nodular cast iron correspond to its microstructure.

4. Conclusion

The European standard for austenitic nodular cast irons specifies the required chemical composition, structure, mechanical and physical properties, but does not prescribe fatigue properties. Therefore, the main aim of the paper was to determine the fatigue resistance of NiMn-grade of austenitic nodular cast iron and to compare it with nodular cast irons with another matrix.

Experiments show that the fatigue limit of austenitic nodular cast iron at alternating symmetrical cyclic push-pull loading is lower than in the case of nodular cast irons with ferrite-pearlitic and pearlite-ferritic matrix. Austenitic nodular cast iron also has a smaller area of the Smith fatigue diagram (the area of safe loading at different types of cyclic loading) than in the case of nodular cast irons with ferrite-pearlitic and pearlite-ferritic matrix. This results in a lower fatigue resistance of austenitic nodular cast iron. This is related to the lower value of the tensile strength, which depends on the microstructure.

Comparison of austenitic (NiMn-grade), ferrite-pearlitic (SiMo-grade) and pearlite-ferritic (SiCu-grade) nodular cast irons shows that in this order, yield strength, tensile strength, hardness and fatigue limit increase, but elongation, reduction of area and absorbed energy decrease.

Austentitic nodular cast iron has lower strength and fatigue properties but excellent plasticity. However, it has many other advantages, especially high resistance to aggressive corrosive environments and oxidation, possibility of use at low or high temperatures and possibility of use for non-magnetic castings.

Acknowledgement

The research has been supported by the Scientific Grant Agency of Ministry of Education, Science, Research and Sport of Slovak Republic, grant project VEGA No. 1/0398/19 and by the Culture and Educational Grant Agency of Ministry of Education, Science, Research and Sport of Slovak Republic, grant project KEGA No. 016ŽU-4/2020.

REFERENCES

[1] S. Věchet, J. Kohout, O. Bokůvka, Fatigue Properties of Ductile Cast Iron, EDIS, Žilina, Slovakia (2002).
[2] O. Bokůvka, G. Nicoletto, M. Guagliano, L. Kunz, P. Palček, F. Nový, M. Chalupová, Fatigue of Materials at Low and High Frequency Loading, EDIS, Žilina, Slovakia (2014).
[3] Giessereilexikon, https://www.giessereilexikon.com/en, accessed: 15.6.2022
[4] D.M. Stefanescu, ASM Handbook **1A**: Cast Iron Science and Technology, ASM International, Materials Park, USA (2017).
[5] K. Röhrig, Konstruieren + Giessen **29** (2), 2-33 (2004).
[6] V. Kaňa, Slévárenství **65** (1-2), 6-11 (2017).
[7] H. Berns, W. Theisen, Ferrous Materials: Steel and Cast Iron, Springer, Bochum, Germany (2008).
[8] S. Franke, Pocket Guide Foundry, Schiele & Schön, Berlin, Germany (2015).
[9] S. Franke, Giesserei-Lexikon, Schiele & Schön, Berlin, Germany (2019).
[10] J.R. Davis, ASM Specialty Handbook: Cast Irons, ASM International, Materials Park, USA (1999).
[11] N. Fatahalla, A. AbuElEzz, M. Semeida, Materials Science and Engineering A **504**, 81-89 (2009).
[12] M.M. Rashidi, M.H. Idris, Materials Science and Engineering A **574**, 226-234 (2013).
[13] M.M. Rashidi, M.H. Idris, Materials Science and Engineering A **597**, 395-407 (2014).
[14] E. Guzik, D. Kopycinski, Archives of Foundry **4** (12), 115-120 (2004).
[15] A. Tabor, P. Putyra, K. Zarebski, T. Maguda, Archives of Foundry Engineering **9** (1), 163-168 (2009).
[16] D. Medyński, A. Janus, S. Zaborski, Archives of Foundry Engineering **17** (1), 121-126 (2017).
[17] Y.X. Zhou, Y.D. Qu, K. Jiang, R.D. Li, Zhuzao/Foundry **66** (10), 1095-1099 (2017).
[18] M. Shi, D.L. Xu, Y. Tian, Y.L. Xiong, Zhuzao/Foundry **67** (1), 62-65 (2018).
[19] R. Singh, T. Matsuo, K. Hayashi, M. Endo, International Journal of Fatigue **163**, 107015 (2022).
[20] P. Skočovský, A. Vaško, Quantitative Evaluation of Structure of Cast Irons, EDIS, Žilina, Slovakia (2007).
[21] J. Belan, L. Kuchariková, E. Tillová, D. Závodská, M. Chalupová, Polytechnica Transportation Engineering **47** (4), 335-341 (2019).
[22] P. Kopas, M. Vaško, M. Handrik, Applied Mechanics and Materials **474**, 285-290 (2014).
[23] I. Pobočíková, Z. Sedliačková, Communications **14**, 88-93 (2012).
[24] A. Vaško, Materials Today: Proceedings **32**, 168-173 (2020).